

Magnetic Properties of $\text{CoFe}_{0.5}\text{Cr}_{1.5}\text{O}_4$ Nanoparticles

G. Márquez^a, V. Sagredo^a, C. Marquina^b, T.E. Torres^{b,c}, M.R. Ibarra^{b,c} and G.F. Goya^c

^aLab. de Magnetismo, Dpto. de Física, Facultad de Ciencias,
Universidad de Los Andes, 5101 Mérida, Venezuela.

e-mail: gersonmarquez@ula.ve

^bInstituto de Ciencia de Materiales de Aragón,
Universidad de Zaragoza-CSIC, E-50009 Zaragoza, Spain.

^cInstituto de Nanociencia de Aragón,
Universidad de Zaragoza, E-50009 Zaragoza, Spain.

Recibido el 25 de junio de 2010; aceptado el 22 de marzo de 2011

Nanoparticles of $\text{CoFe}_{0.5}\text{Cr}_{1.5}\text{O}_4$ were synthesized by using the auto-combustion method. Structural and magnetic properties were particularly investigated. The obtained powder was characterized by X-ray diffraction (XRD) and magnetic measurements as a function of temperature and applied magnetic field. X-ray diffraction data suggested the presence of single crystalline phase corresponding to cubic-spinel structure. The size particle was estimated by the Scherrer equation in 23 nm. The main characteristic of the Field Cooling (FC) and Zero Field Cooling (ZFC) curves is the presence of a magnetic transition at about 175 K; below this temperature the compound is magnetically ordered, as ferrimagnetic state, and above 175 K the magnetic behavior of the system is suggested that superparamagnetic. At 5 K the mixed oxide presents a quite high coercive field, 5.8 kOe.

Keywords: Spinel; nanoparticles; superparamagnetism.

Nanopartículas de $\text{CoFe}_{0.5}\text{Cr}_{1.5}\text{O}_4$ fueron sintetizadas mediante el método de auto-combustión. Las propiedades estructurales y magnéticas fueron especialmente estudiadas. Los polvos obtenidos fueron caracterizados mediante difracción de rayos-X (XRD) y medidas magnéticas en función de la temperatura y del campo magnético aplicado. El perfil de difracción de rayos-X sugiere la presencia de una sola fase cristalina correspondiente a la estructura cúbica espinela. El tamaño de las partículas fue estimado mediante la ecuación de Scherrer, obteniendo tamaños de partícula de 23 nm. La característica principal de las curvas de magnetización, Field Cooling (FC) y Zero Field Cooling (ZFC), es la presencia de una transición magnética alrededor de 175 K; por debajo de esta temperatura el compuesto se encuentra magnéticamente ordenado, en estado ferrimagnético, y por encima de 175 K el comportamiento magnético del sistema se sugiere es superparamagnético. A 5 K el óxido mixto presenta un considerable campo coercitivo de 5,8 kOe.

Descriptores: Espinela; nanopartículas; superparamagnetismo.

PACS: 61.05.cp; 61.46.Df; 75.50.Gg; 75.50.Tt.

1. Introduction

Nanosized spinel mixed oxides, such as ferrites and chromites, have been extensively studied because of important physical and chemical properties that make these materials are interesting for their high number of applications as high-density information storage, catalysts, ferrofluids, sensors, biomedical treatments, etc [1-4]. Very recently it has been found that the cobalt chromite (CoCr_2O_4) nanostructured presents very interesting magnetic and catalytic properties. One of the possible applications is the elimination of NO_x gases produced in the emission exhaust from diesel vehicles [2,5].

The cobalt chromite crystallizes in the well known cubic-spinel structure with general formula AB_2O_4 . The spinel structure presents two possible arrangements: the first one known as normal spinel is characterized by A cations in the tetrahedral sites and B cations in the octahedral positions. A second possible arrangement known as inverse spinel, in which the A cations occupies one half of the octahedral co-

ordination sites and the B cations occupies the other half of the octahedral sites as well as all of the tetrahedral positions. However, there are many possible intermediate distributions represented by the formula $(\text{A}_{1-\lambda}\text{B}_\lambda)^T(\text{A}_\lambda\text{B}_{2-\lambda})^O\text{O}_4$ where λ is called inversion parameter [6]. On the other hand, the bulk cobalt chromite presents a magnetic transition around 93 K [7-9].

Nanosize spinel oxides have been prepared by various techniques such as sol-gel, combustion, coprecipitation, hydrothermal process, ball milling and the microemulsion method [10-12].

We have considered quite interesting the partial substitution of Cr^{+3} by Fe^{+3} in the nano-cobalt chromite and carry out an study on the structural and magnetic changes because of the interactions between those three magnetic ions: Co^{+2} , Fe^{+3} and Cr^{+3} . For this reason, nanoparticles of $\text{CoFe}_{0.5}\text{Cr}_{1.5}\text{O}_4$ were synthesized by using the auto-combustion method, with nitrates of the cations as the precursors and urea as fuel.

In this work we report on the structure and magnetic properties of $\text{CoFe}_{0.5}\text{Cr}_{1.5}\text{O}_4$ nanoparticles.

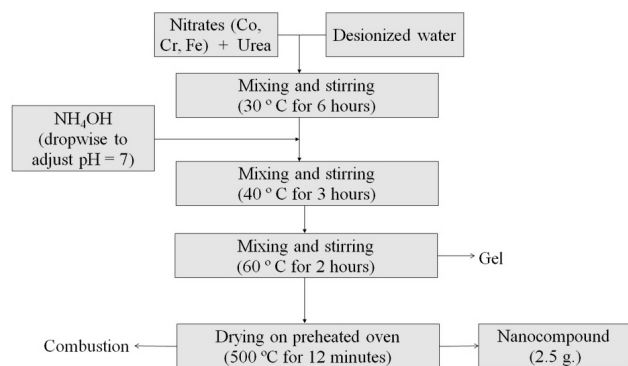


FIGURE 1. Schematic representation of synthesis method of $\text{CoFe}_{0.5}\text{Cr}_{1.5}\text{O}_4$ nanocompound.

2. Experimental

Nanoparticles of $\text{CoFe}_{0.5}\text{Cr}_{1.5}\text{O}_4$ were obtained by the auto-combustion method. To get 2.5 grams of final compound, stoichiometric quantities of nitrates: $\text{Co}(\text{NO}_3)_2 \cdot 6\text{H}_2\text{O}$, $\text{Fe}(\text{NO}_3)_3 \cdot 9\text{H}_2\text{O}$ and $\text{Cr}(\text{NO}_3)_3 \cdot 9\text{H}_2\text{O}$, and urea $\text{CO}(\text{NH}_2)_2$, were dissolved in desionized water following the procedure schematically illustrated in Fig. 1. The amount of urea used is determined by adjusting the stoichiometric coefficient $\phi=1.5$, according to the method proposed by Jain *et al.* [13].

During constant stirring, ammonium hydroxide (NH_4OH) was added dropwise to get a solution with pH about 7, starting with the precipitation of the final compound.

The obtained powder was characterized by X-ray diffraction (XRD) using a D/Max Rigaku powder diffractometer equipped with a rotating anode and a graphite monochromator to select $\text{CuK}\alpha$ radiation to identify the crystalline phases present in the samples. Using the data from the pattern of X-ray diffraction, particle size was estimated by the Scherrer equation [14]:

$$D = \frac{0.9\lambda}{\beta \cos \theta} \quad (1)$$

where D is the particle size, λ is the wavelength of X-rays, β is the half width of intensity maximum peak and θ is the diffraction angle.

The magnetic measurements were made using a SQUID magnetometer, MPMS-XL5 of Quantum Design, in the temperature range from 5K to 300K and applying a magnetic field up to 50 kOe. In addition, we used a Vibrating Sample Magnetometer EV7 of ADE TECHNOLOGIES to measure hysteresis loops at room temperature by applying a magnetic field up to 20 kOe.

3. Results and discussion

The XRD patterns of the sample of $\text{CoFe}_{0.5}\text{Cr}_{1.5}\text{O}_4$ nanoparticles synthesized is presented in Fig. 2. Comparing the obtained diffractogram with the patterns of the international crystallographic cards of CoCr_2O_4 and CoFe_2O_4 (JCPDS: 22-1084 y JCPDS: 22-1086) [15,16], it is found that all the

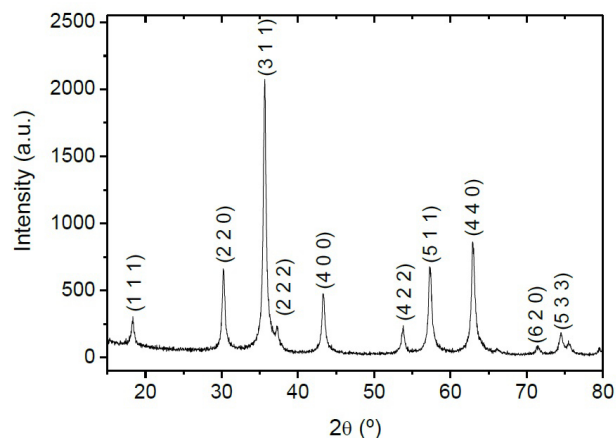


FIGURE 2. Indexed X-ray diffraction pattern of $\text{CoFe}_{0.5}\text{Cr}_{1.5}\text{O}_4$ nanoparticles.

observed intensity maxima correspond to the characteristic peaks of CoCr_2O_4 and CoFe_2O_4 . This means that the sample correspond to a single crystalline phase: the cubic-spinel structure.

It was found that the unit cell parameter of $\text{CoFe}_{0.5}\text{Cr}_{1.5}\text{O}_4$ is 8.347 (1) Å, slightly larger than the known to the CoCr_2O_4 (8.3299 Å) as observed by Mane *et al.* [17]. This result is reasonable since it is replacing part of the cations Cr^{+3} by Fe^{+3} in the cobalt chromite, and also ionic radius of Fe^{3+} (0.645Å) is higher than the Cr^{3+} (0.63 Å) [18]. On the other hand, the average particle size estimated by the Scherrer's equation is approximately 23 nm.

In Fig. 3 we show the measures Field Cooling (FC) and Zero Field Cooling (ZFC) magnetization of cobalt-chromite. Here we can see that there is a magnetic transition at about 175 K, above this temperature the nanocompound is in a disordered magnetic state (superparamagnetic state). In the range of temperatures below 175 K, the compound is magnetically ordered (ferrimagnetic state).

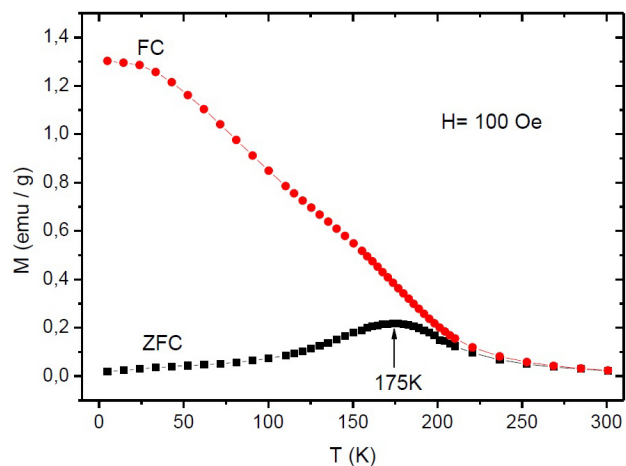


FIGURE 3. Temperature dependence of the FC and ZFC magnetization.

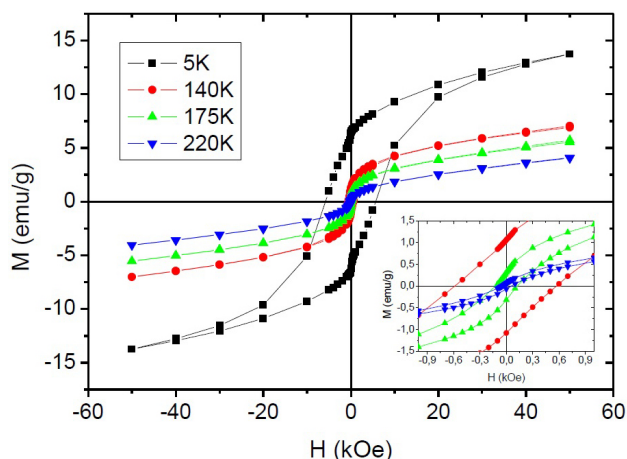


FIGURE 4. Field dependence of magnetization curves for $\text{CoFe}_{0.5}\text{Cr}_{1.5}\text{O}_4$ nanocompound at different temperatures.

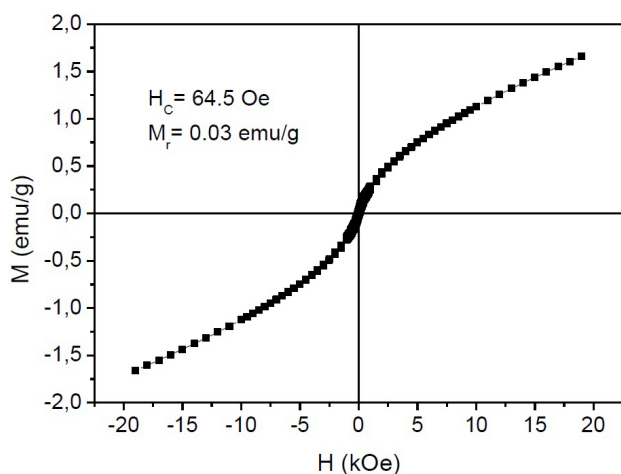


FIGURE 5. Field dependence of magnetization for $\text{CoFe}_{0.5}\text{Cr}_{1.5}\text{O}_4$ particles at room temperature.

Figure 4 shows the isothermal magnetization curves measured at 5 K, 140 K, 175 K and 220 K, we can observe that the M-H curve at 220 K shows a similar behavior to that of a superparamagnetic system, what makes us infer that at 220 K the $\text{CoFe}_{0.5}\text{Cr}_{1.5}\text{O}_4$ sample is in a superparamagnetic state, which is consistent with the results obtained in the measurements of FC and ZFC magnetization. At 5 K we can see a clear hysteresis loop with a coercive field of 5.8 kOe. In Fig. 4 can be also noted that in the different M-H curves, the magnetization does not reach saturation with the maximum applied magnetic field (50 kOe), therefore in Table I instead of the saturation magnetization we refer to the magnetization measured with the maximum applied magnetic field as the maximum magnetization (M_m).

TABLE I. Magnetic parameters of the $\text{CoFe}_{0.5}\text{Cr}_{1.5}\text{O}_4$ nanoparticles.

T (K)	H_c (Oe)	M_r (emu/g)	M_m (emu/g)
5	5800	6.40	13.7*
140	585	1.06	7.0*
175	123.3	0.31	5.7*
220	50.1	0.07	4.1*
300	64.5	0.03	1.7**

*Magnetic field up to 50 kOe, **Magnetic field up to 20 kOe

It is possible to notice in Fig. 4 that the coercivity of the nanoparticles decreases as the temperature increases toward the blocking temperature. The inserts in Fig. 4 show the part of the $M(H)$ loops in the region of small applied field. Figure 5 shows the hysteresis curve at room temperature, as in the M-H curve at 220 K is similar to the behavior of a superparamagnetic system.

Table I shows the magnetic parameters of the nanocompound under study, where we can see that the values of coercive field (H_c), remanent magnetization (M_r) and maximum magnetization (M_m) at 5 K are greater than those found in measurements made at higher temperatures (140 K, 175 K, 220 K and 300 K). In addition, it is possible to see that the value of these parameters decreases with increasing temperature towards the magnetic transition temperature (175 K), a result which agrees with the findings on measures of FC and ZFC magnetization.

4. Conclusions

$\text{CoFe}_{0.5}\text{Cr}_{1.5}\text{O}_4$ nanoparticles synthesized by auto-combustion method has a single crystalline phase corresponding to the cubic-spinel structure. The average particle size estimated by Scherrer equation was 23 nm. The curves of magnetization as a function of temperature (FC and ZFC) and depending on the applied magnetic field showed that $\text{CoFe}_{0.5}\text{Cr}_{1.5}\text{O}_4$ presents a magnetic transition around 175K. Below this temperature the compound shows a ferrimagnetic behavior and above 175 K it is in the superparamagnetic state.

Acknowledgements

G. Márquez and V. Sagredo are thankful to CDCHT-ULA for providing financial support for this work through the projects: C-1641-08-05-ED and C-1658-09-05-A.

1. Q.A. Pankhurst, J. Connolly, S.K. Jones and J. Dobson, *J. of Phys. D: Appl. Phys.* **36** (2003) R167.
2. D. Fino, N. Russo, G. Saracco and V. Specchia, *J. of Catalysis* **242** (2006) 38.
3. M. Tada, S. Hatanaka, H. Sanbonsugi, N. Matsushita and M. Abe, *J. Appl. Phys.* **93** (2003) 7566.
4. D-H. Kim, S-H. Lee, K-N. Kim, K-M. Kim, I-B. Shim and Y-K. Lee, *J. Magn. Magn. Mater.* **293** (2005) 320.
5. D. Fino, N. Russo, G. Saracco and V. Specchia, *Powder Technology* **180** (2008) 74.
6. D. S. Mathew and R-S. Juang, *Chem. Eng. J.* **129** (2007) 51.
7. Y. Yamasaki, S. Miyasaka, J.P. He, T. Arima and Y. Tokura, *Phys. Rev. Lett.* **96** (2006) 207204.
8. N. Menyuk, K. Dwight and A. Wold, *J. Phys. (Paris)* **25** (1964) 528.
9. K. Tomiyasu, J. Fukunaga and H. Suzuki, *Phys. Rev. B* **70** (2004) 214434.
10. A.F. Júnior, E.C. de Oliveira Lima, M.A. Novak and P.R. Wells Jr, *J. Magn. Magn. Mater.* **308** (2007) 198.
11. C. Cannas, A. Musinu, D. Peddis and G. Piccaluga, *J. of Nanoparticle Research* **6** (2004) 223.
12. Taeghwan Hyeon, *Chem. Commun.* (2003) 927.
13. S.R. Jain, K.C. Adiga, and V.R.P. Verneker, *Combust. Flame* **40** (1981) 71.
14. A.L. Patterson, *Phys. Rev.* **56** (1939) 978.
15. Joint Committee on Powder Diffraction Standards (JCPDS) - International Centre for Diffraction Data: 22-1084 (1971).
16. Joint Committee on Powder Diffraction Standards (JCPDS) - International Centre for Diffraction Data: 22-1086 (1971).
17. D.R. Mane, U.N. Devatwal and K.M. Jadhav, *Mater. Lett.* **44** (2000) 91.
18. K.P. Chae, Y.B. Lee, J.G. Lee, and S.H. Lee, *J. Magn. Magn. Mater.* **220** (2000) 59.